Thin-Film Lithium Niobate Modulators With Angled Electrodes for Improved Modulation Efficiency

Xi Chen
Guangdong Provincial Key Laboratory of Optical Fiber Sensing and Communications, Institute of Photonics Technology, Jinan University
Guangzhou, China
chenxi08@stu2021.jnu.edu.cn

Hongwei Li
Guangdong Provincial Key Laboratory of Optical Fiber Sensing and Communications Institute of Photonics Technology, Jinan University
Guangzhou, China
lihongwei@stu2021.jnu.edu.cn

Kun Zhang
Guangdong Provincial Key Laboratory of Optical Fiber Sensing and Communications Institute of Photonics Technology, Jinan University
Guangzhou, China
kzhang@jnu.edu.cn

Jiejun Zhang*
Guangdong Provincial Key Laboratory of Optical Fiber Sensing and Communications Institute of Photonics Technology, Jinan University
Guangzhou, China
zhangjiejun@jnu.edu.cn

Jianping Yao
Faculty of Engineering University of Ottawa
Ottawa, ON K1N6N5, Canada
Institute of Photonics Technology, Jinan University
Guangzhou, China
jpyao@jnu.edu.cn

***Abstract*—Low-power electro-optic modulators are crucial devices for applications such as data center communications. In this work, we report a design featuring a traveling wave electrode with a sidewall angle and an optical slot waveguide to reduce the driving voltage of an electro-optic modulator. The design of our electro-optic modulator is based on matured semiconductor processing technology, which is commonly used in the fabrication of optical devices. Through the optimization of the angle of the electrode sidewall, the electric field concentration near the optical waveguide is strongly enhanced, and therefore the overlap between the electric field and optical field is increased. We achieve a voltage-length product of 1.48 V·cm and a 3-dB modulation bandwidth of over 200 GHz. Our results demonstrate that the angled electrode design exhibits superior performance in terms of increased modulation efficiency and reduced electrode size compared to traditional traveling wave electrodes. This approach has the potential to be extended to electro-optic modulators of other structures.**

Keywords—electrooptical modulator, thin film lithium niobate, traveling wave electrode

INTRODUCTION

As data centers continue to evolve in response to the growing demand for cloud computing and 5G networks, devices used in these centers must adapt to meet the changing needs of these environments [1]. Electro-optical modulators, which are critical components for electro-optical conversion, must also evolve to meet the demands of lower power consumption and higher speed operation [2]. In recent years, various material platforms have been developed for high-performance electro-optic modulators, including bulk lithium niobate [3], indium phosphide (InP) [4], and silicon-on-insulator [5]. Among these, thin-film lithium niobate (TFLN) platforms have shown particular promise for meeting the needs of electro-optic conversion devices in data centers [6].

In 2018, the first high-performance TFLN electro-optic modulator was demonstrated [7], achieving a 4.4-V half-wave voltage and 3-dB electro-optical bandwidth of 100 GHz with a modulator length of 5 mm. In 2019, a hybrid LN/Si integrated electro-optic modulator with a length of 5 mm was demonstrated to achieve a 5.1 V half-wave voltage and a 70 GHz bandwidth [8]. However, a trade-off between the half-wave voltage and the bandwidth has to be made for those modulators. One approach to achieving a large electro-optical bandwidth in those modulator design without increasing the half-wave voltage is to use a segmented electrode design [9-10]. However, the segmented electrode design requires using quartz substrate for the TFLN substrate, which may increase the cost of the device. On the other hand, to reduce the half-wave voltage without reducing the bandwidth, one approach is to perform shallow etching of the lithium niobate ridge waveguide, or the use of silicon nitride [11] or silicon [12] on a TFLN to increase the proportion of the optical field in the lithium niobate medium. In addition to the travelling-wave modulation, a resonant cavity [13], a Bragg grating [14] or a photonic crystal waveguide [15] may also be used to significantly reduce the optical group velocity, thus increasing the interaction time between the electric and optical fields within a limited device length. However, such devices have a limited optical bandwidth and are sensitive to temperature.

In this work, a TFLN modulator based on a slot waveguide to increase the optical confinement and a traveling-wave electrode with an angled sidewall to reduce the half-wave voltage is studied. The impact of the electrode sidewall angle on the optical waveguide loss, the microwave refractive index, and the electrical impedance of the modulator is investigated theoretically and numerically. By optimizing the sidewall angle of the electrodes, a TFLN modulator is achieved with a voltage-length product of 1.48 V cm, in which 3-dB modulation bandwidths of 200 GHz and 120 GHz are achieved with modulator lengths of 3 mm and 5 mm. The introduction of an angled electrode in a TFLN modulator provides an additional degree of freedom for the realization of the modulator with a lower drive voltage, larger electro-optical bandwidth, and smaller size. Additionally, the electro-optic modulator we design utilizes a well-established

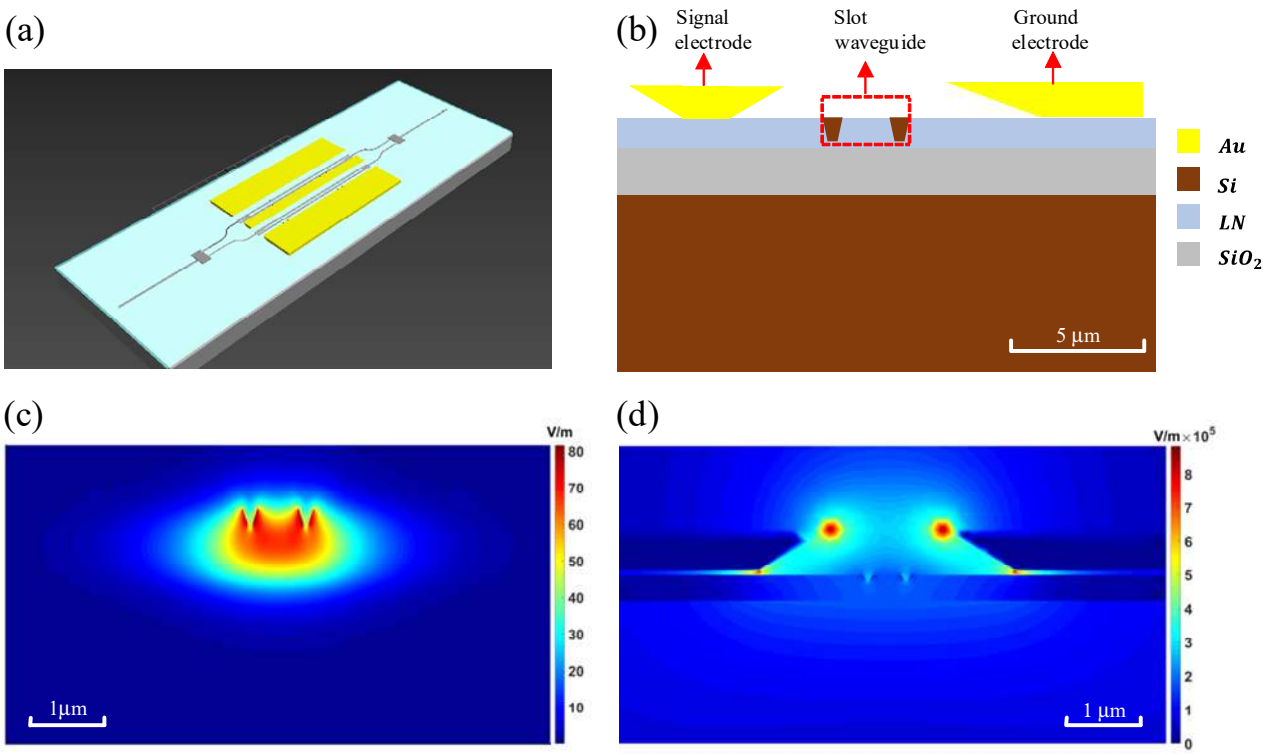

FIG.1 (a) Three-dimensional view of the modulator, (b) modulator cross section, (c) optical field distribution, and (d) electric field distribution.

semiconductor processing technology. Specifically, the electrode processing with the required angle featured in our design is a commonplace technique widely employed in the processing of blazed gratings [16].

PRINCIPLE

The design of a low half-wave voltage TFLN electro-optic modulator is shown in Fig. 1(a). The modulator has a Mach-Zehnder interferometer (MZI) structure, in which two multimode interference (MMI) couplers are used to split and combine the light waves to and from the two MZI arms. Two push-pull phase modulators with each having an angled electrode for an improved modulation efficiency are incorporated in the two arms of the MZI. By adjusting the sidewall angles of the electrodes, the modulator is optimized to operate at a low driving voltage.

In the design, two strips with a high refractive index (Si) are used to form a slot waveguide, with a low refractive index material (lithium niobate or LN) wrapping around and filling the resulting slot. We incorporate two silicon slots within the TFLN to form a slot structure of Si-LN-Si, as depicted in the dashed box in Fig. 1(b). The vertical slot structure can efficiently guide the TE light waves with a high optical confinement [18], as shown by the simulated optical field distribution in Fig. 1(c). A large fraction of the optical field is confined within the LN, thus maximizing the utilization of its high electro-optical coefficient. On the other hand, the electric field distribution excited by the angled electrode is shown in Fig. 1(d). The utilization of angled electrodes, as opposed to vertical ones, results in a reduction in the distance between the electrodes for a fixed spacing, leading to an increased concentration of the electric field in the vicinity of the optical waveguide. The voltage-length product is given by [18],

$$V_\pi L = \frac{n_{eff}\lambda_0 G}{2n_e^{\,4}\gamma_{33}\tau} \tag{1}$$

where G is the gap between electrodes, n_{eff} is the effective mode refractive index of the LN at λ_0, n_e is the refractive index of the LN for an extraordinary light traveling in the LN, and γ_{33} is the electro-optical coefficient of the LN, τ is the electro-optic overlap factor, which is used to indicate the extent of overlap between the electric field and the optical field. When the electrode spacing is a constant, an increase in the overlap between the electric field and the optical field leads to a decrease in the voltage-length product. The implementation of electrodes with sidewall angles and slot waveguides in our design serves to enhance the overlaps between the electric field and the optical field.

Another crucial parameter of the electro-optic modulator is the electro-optic bandwidth. The frequency response of a Mach-Zehnder modulator with a traveling wave electrode can be expressed as [19]:

$$m(\omega) = \left| \frac{2Z_{in}}{Z_{in}+50} \frac{(50+Z_0)F(u_+)+(50-Z_0)F(u_-)}{(50+Z_0)e^{\gamma_m L}+(50-Z_0)e^{-\gamma_m L}} \right| \tag{2}$$

where Z_{in} is the input microwave impedance of the device and Z_0 is the characteristic impedance of the traveling wave electrode, γ_m is the propagation constant of microwave in the gold electorde. $F(u_\pm) = \left(1 - exp(u_\pm)\right)/u_\pm$ and $u_\pm = \pm\alpha_m L + j\omega\left(\pm\left(n_m - n_g\right)\right)L/c$, ω is the angular frequency of the light wave, L is the length of the modulation region, c is the speed of light in vacuum, and α_m, n_m and n_g are,

respectively, the microwave loss, the microwave effective refractive index and the optical effective refractive index.

To determine the two key parameters of the modulator, namely the microwave bandwidth and the half-wave voltage, at a working wavelength of 1550 nm, we performed a microwave mode distribution analysis on the single-arm section of the modulator, as illustrated in Figure 1(b), utilizing commercially available simulation software HFSS. The characteristic impedance, microwave refractive index, and other parameters are derived from this analysis. we utilize COMSOL to calculate the distribution of the optical field and electric field within the modulation region, and subsequently utilize Eq. (1) to determine the voltage-length product.

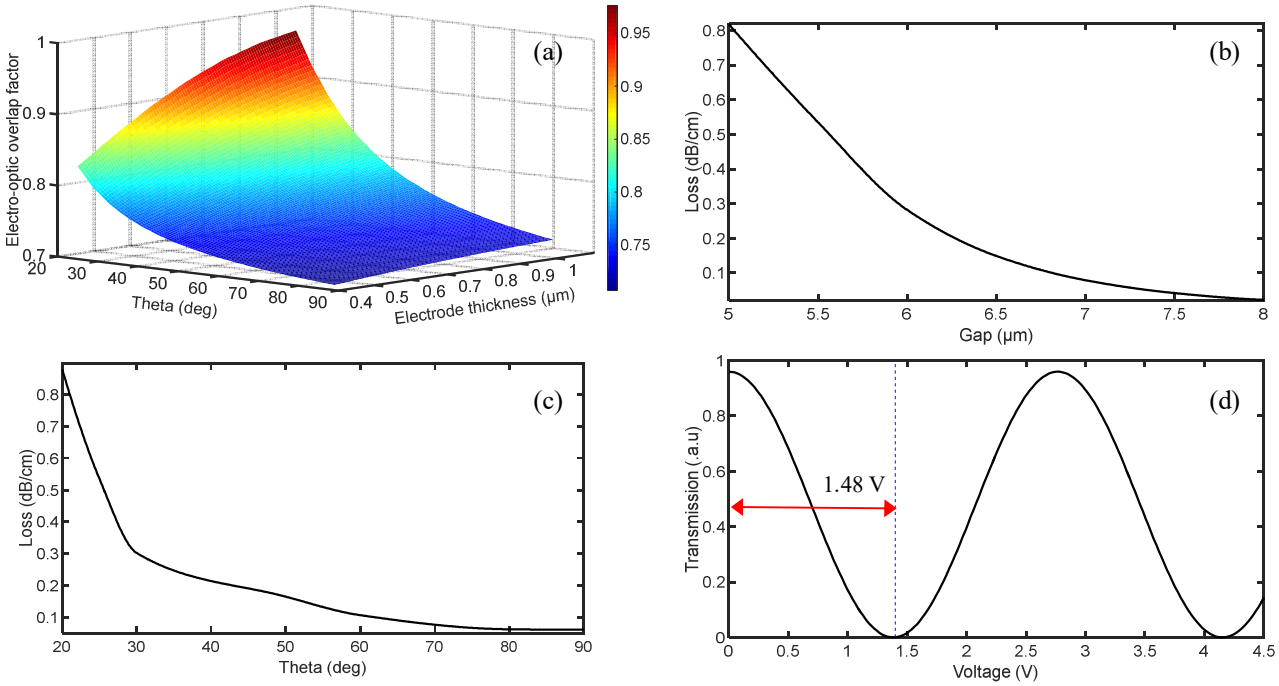

FIG. 2 (a) The overlap factor between the electric and optical field in the modulation region as functions of the electrode sidewall angle and thickness, (b) the relationship between the electrode gap and optical waveguide loss, (c) the relationship between the electrode sidewall angle and the optical waveguide loss and, (d) the normalized voltage-transmission relationship

RESULT AND DISCUSSION

As demonstrated in Fig 2(a), the thickness of the electrode and the angle of the electrode sidewall significantly affect the overlap factor between the electric field and optical field. An increase in electrode thickness from 0.4 μm to 1 μm results in a 0.25 increase in the overlap factor, while a decrease in the angle of the electrode sidewall from 90 to 20 degrees also leads to an increase in the overlap factor. The inclusion of this design parameter in the electrode allows for a decrease in the voltage-length product. Furthermore, as depicted in Fig. 2(b), the optical loss caused by the metal electrodes must be taken into account. It is desirable to minimize optical loss in order to facilitate the cascading and large-scale implementation of the device. The optical loss caused by metal is reduced as the electrode spacing is increased, as shown in Fig. 2(c). However, as shown in Fig. 2(d), a smaller angle of the electrode sidewall leads to a higher loss of optical energy. Through careful optimization of the design parameters, an exceptionally low half-wave voltage-length product of 1.48 V cm is achieved.

To achieve a large electro-optic response bandwidth, an ideal design should be performed, to minimize microwave transmission loss, to achieve impedance match between the transmission line and an external input device, and to match the refractive indices (velocities) of the microwave transmission line with the that of the optical gap waveguide. To achieve this, a coordinated design of the entire system is necessary. In our simulation, we use a standard TFLN wafer, which may impose certain limitations on some parameters such as the thickness of the TFLN (600 nm), the thickness of the underlying silica (2 μm/4.7 μm), and thickness of the silicon substrate (500 μm). Additionally, the deposition thickness of the metal electrode is limited to a maximum valvalueue of 1.1 μm due to technological constraints.

Finally, we undertake an optimization process to refine the overall design of the modulator and present the resulting parameters of the transmission line in Fig. 3(a). In terms of characteristic impedance, the transmission line maintains an impedance of approximately 49±0.5 Ω from 10 to 200 GHz, which is close to a designed value of 50 Ω. As shown in Fig 3(b), the refractive index of the microwave transmission line is approximately 2.2±0.1 from 20 to 200 GHz, which aligns well with the group refractive index of 2.2 of the LN. In terms of microwave loss, as shown in Fig. 3(c), the narrow electrode spacing of 5.5 μm is balanced with other design parameters to make the microwave loss small. As shown in Fig. 3(d), the 3-dB electro-optical modulation bandwidth is 120 GHz at a modulation length of 5 mm, 170 GHz at a modulation length of 4 mm, and exceeds 200 GHz at a modulation length of 3 mm.

CONCLUSION

We demonstrated an electro-optic modulator based on Si on LN platform. By using slot waveguides with optimized angles of the electrodes, the voltage-length product was

reduced while maintaining a large electro-optic response bandwidth. A voltage-length product of 1.48 V·cm and a 3 dB electro-optic response bandwidth of more than 200 GHz were achieved in our design. We should emphasize that the design was performed using the parameters of a commercial TFLN wafer, which is ready for device fabrication. We believe that the low voltage-length product of the design would contribute to the implementation of electro-optic modulators with significantly increased performance.

ACKNOWLEDGMENT

This work was supported by the National Key R&D Program of China (2021YFB2800804), National Natural Science Foundation of China (61860206002) and the Guangdong Province Key Field R&D Program Project (2020B0101110002).

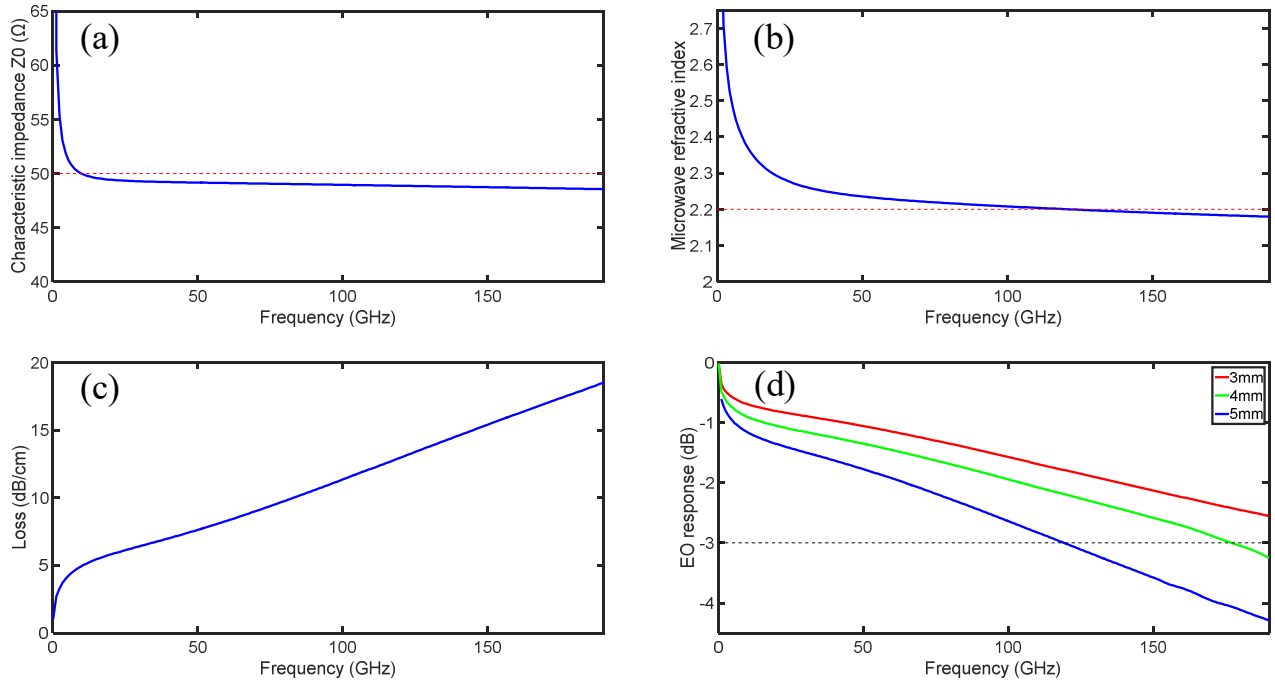

FIG. 3 (a) Simulated characteristic impedance, (b) simulated microwave refractive index, (c) simulated microwave loss, and (d) electro-optical response bandwidth

REFERENCES

[1] P. J. Winzer, D. T. Neilson, and A. R. Chraplyvy, "Fiber-optic transmission and networking: the previous 20 and the next 20 years," Opt. Express, vol. 26, no. 18, pp. 24190–24239, 2018.

[2] Q. Cheng, M. Bahadori, M. Glick, S. Rumley, and K. Bergman, "Recent advances in optical technologies for data centers: a review," Optica, vol. 5, no. 11, pp. 1354–1370, 2018.

[3] E. L. Wooten et al., "A review of lithium niobate modulators for fiber-optic communications systems," Ieee J Sel Top Quant, vol. 6, no. 1, pp. 69–82, 2000.

[4] R. A. Griffin, S. K. Jones, N. Whitbread, S. C. Heck, and L. N. Langley, "InP Mach–Zehnder modulator platform for 10/40/100/200-Gb/s operation," Ieee J Sel Top Quant, vol. 19, no. 6, pp. 158–166, 2013.

[5] C. E. Png, S. P. Chan, S. T. Lim, and G. T. Reed, "Optical phase modulators for MHz and GHz modulation in silicon-on-insulator (SOI)," J. Light. Technol., vol. 22, no. 6, p. 1573, 2004.

[6] https://www.accesswire.com/692542/Eoptolink-Pushes-Lower-Power-Limits-for-400G-and-800G-Transceivers-at-OFC-2022

[7] C. Wang et al., "Integrated lithium niobate electro-optic modulators operating at CMOS-compatible voltages," Nature, vol. 562, no. 7725, pp. 101–104, 2018.

[8] M. He et al., "High-performance hybrid silicon and lithium niobate Mach–Zehnder modulators for 100 Gbit s- 1 and beyond," Nat. Photonics, vol. 13, no. 5, pp. 359–364, 2019.

[9] M. Xu et al., "Dual-polarization thin-film lithium niobate in-phase quadrature modulators for terabit-per-second transmission," Optica, vol. 9, no. 1, pp. 61–62, 2022.

[10] P. Kharel, C. Reimer, K. Luke, L. He, and M. Zhang, "Breaking voltage–bandwidth limits in integrated lithium niobate modulators using micro-structured electrodes," Optica, vol. 8, no. 3, pp. 357–363, 2021.

[11] A. Honardoost, F. A. Juneghani, R. Safian, and S. Fathpour, "Towards subterahertz bandwidth ultracompact lithium niobate electrooptic modulators," Opt. Express, vol. 27, no. 5, pp. 6495–6501, 2019.

[12] J. Wang, H. Yang, and W. Zou, "Engineering a sandwiched Si/I/LNOI structure for 180-GHz-bandwidth electro-optic modulator with fabrication tolerances," Opt. Express, vol. 30, no. 20, pp. 35398–35408, 2022.

[13] B. Pan et al., "Compact electro-optic modulator on lithium niobate," Photonics Res, vol. 10, no. 3, pp. 697–702, 2022.

[14] X. Huang, Y. Liu, H. Guan, Z. Yu, M. Tan, and Z. Li, "High-Efficiency, Slow-Light Modulator on Hybrid Thin-Film Lithium Niobate Platform," IEEE Photon. Technol. Lett, vol. 33, no. 19, pp. 1093–1096, 2021.

[15] M. Li, J. Ling, Y. He, U. A. Javid, S. Xue, and Q. Lin, "Lithium niobate photonic-crystal electro-optic modulator," Nat. Commun, vol. 11, no. 1, p. 4123, 2020.

[16] J. Gao, P. Chen, L. Wu, B. Yu, and L. Qian, "A review on fabrication of blazed gratings," J. Phys. D, vol. 54, no. 31, p. 313001, 2021.

[17] C. A. Barrios et al., "Slot-waveguide biochemical sensor," Opt. Lett, vol. 32, no. 21, pp. 3080–3082, 2007.

[18] P. O. Weigel, F. Valdez, J. Zhao, H. Li, and S. Mookherjea, "Design of high-bandwidth, low-voltage and low-loss hybrid lithium niobate electro-optic modulators," Journal of Physics: Photonics, vol. 3, no. 1, p. 012001, 2020.

[19] J. Cai, C. Guo, C. Lu, A. P. T. Lau, P. Chen, and L. Liu, "Design optimization of silicon and lithium niobate hybrid integrated traveling-

wave Mach-Zehnder modulator," IEEE Photon. J., vol. 13, no. 4, pp. 1–6, 2021.